ESD-TDR-65-238

Technical Report

393

C. A. Lindberg

12-Horn Monopulse Antenna System for Millstone Hill Radar

15 June 1965

Prepared under Electronic Systems Division Contract AF 19(628)-500 by

Lincoln Laboratory
MASSACHUSETTS INSTITUTE OF TECHNOLOGY
Lexington, Massachusetts

The work reported in this document was performed at Lincoln Laboratory, a center for research operated by Massachusetts Institute of Technology, with the support of the U.S. Air Force under Contract AF 19(628)-500.

MASSACHUSETTS INSTITUTE OF TECHNOLOGY

LINCOLN LABORATORY

12-HORN MONOPULSE ANTENNA SYSTEM FOR MILLSTONE HILL RADAR

C. A. LINDBERG

Group 61

TECHNICAL REPORT 393

15 JUNE 1965

LEXINGTON MASSACHUSETTS

ABSTRACT

The 440-Mcps conical-scan tracker at the Millstone Hill radar site has been converted to an L-band 12-horn monopulse tracker utilizing a Cassegrain optics reflector system. The amplitude sensing monopulse feed illuminates a 10-foot subreflector and thence an 84-foot-diameter paraboloid with linear or either sense of circular polarization. This system conversion increased the capabilities of the radar complex in that higher antenna gain and increased tracking sensitivity are obtained. The merits of the 12-horn system have been proven with actual results substantiating the theoretical predictions. This report discusses the design considerations and final performance characteristics of the overall antenna system and its individual components.

Accepted for the Air Force
Stanley J. Wisniewski
Lt Colonel, USAF
Chief, Lincoln Laboratory Office

TABLE OF CONTENTS

12-HORN MONOPULSE ANTENNA SYSTEM FOR MILLSTONE HILL RADAR

I. INTRODUCTION

The Millstone Hill antenna system (Figs. 1 and 2) is an amplitude sensing monopulse designed for optimum operation at 1300 ± 50 Mcps. It utilizes twelve pyramidal horns as primary radiators rather than the more conventional four or five horns.

The system is capable of transmitting signals which are either circularly polarized (right- or left-hand sense) or linearly polarized in a vertical direction (Table I). The power handling capability is 5-Mw peak and 150-kw average. A Cassegrain reflector system (Fig. 3) is used to provide more flexibility in feed design and to shorten feed-to-receiver transmission lines. The existing main reflector, which was satisfactory at UHF frequencies, was not sufficiently accurate for this application and was replaced with a more precise paraboloid. An equipment shelter (Fig. 4) containing preamplifiers and associated electronics was also added on the aft section of the azimuth deck (see Fig. 2) to reduce the receive line losses and to provide a convenient location for the low-noise receiving equipment.

II. FEED SYSTEM

A. General

In determining the type of feed to be used in a tracking system, two major considerations are manifested in maximizing the sum channel gain and error sensitivity. In converting the Millstone complex from the UHF band to the higher frequency range, the effectively larger

TABLE I

SYSTEM POLARIZATION
(1250 to 1350 Mcps)

Transmit	Receive	Track
RHCP	RHCP and LHCP	LHCP
LHCP	LHCP and RHCP	RHCP
Vertical	Vertical and Horizontal	Horizontal

antenna aperture provides 10 db more one-way system gain. An additional increase in gain is realized in converting from conical scan to monopulse. An optimized conical-scan feed usually results when the crossover level is set between −1.5 and −3.0 db. The boresight or reference gain is therefore −1.5 to −3.0 db below the maximum gain of a single on-axis beam. On the other hand, an optimum 4-horn monopulse system has a maximum gain approximately 1 db below a single on-axis beam. Since error sensitivity is the product of gain and angular sensitivity, and because the gain is improved over that of a conical-scan system, it follows that the error sensitivity is also improved.

B. Theoretical Advantages of a 12-Horn System

A 4- or 5-horn system can usually be designed "satisfactorily" for most applications. However, sum channel gain and angular sensitivity must be compromised, because they are not optimum for the same feed configuration. Two methods which have been proposed in the past to improve this condition are a multimode network and a multihorn system (horns in excess of five). It was decided to investigate further the multihorn system[1] and then to design and fabricate a feed network to fulfill the requirements of the Millstone radar.

A study was made of 4-, 5-, and 12-horn arrays to determine the optimum aperture sizes necessary to illuminate a 10-foot-diameter subreflector. This size hyperboloid was chosen as a starting point; it was not too large mechanically or too small electrically. (A small diameter hyperboloid requires a relatively large horn aperture for proper illumination.) It was found that a 4-horn system with 1.65-wavelength apertures would provide near optimum sum channel gain but that the error sensitivity was down approximately 4 db from that obtainable with a 12-horn system. The optimum 5-horn system had objectionably high sidelobes in the error pattern and a relatively low error sensitivity caused by the inherent wide separation between outside horns. This separation is determined by the aperture of the sum channel horn required in the center.

The 12-horn system provides four center horns very nearly equal to the optimum size for maximum boresight gain. To each exterior wall of these horns is added one additional horn. The comparator (Figs. 5 and 6) is designed so that these horns are combined, both in phase and amplitude, with the four center horns to form the required difference patterns. The advantage over the 4-horn system is that with the additional horns one can produce primary sum and difference patterns which result in essentially equally efficient illumination of the main reflector. The gain of both the sum and difference channels is thus optimum. Because the error sensitivity is dependent upon the gain and the squint angle of the error beams, and angular sensitivity is proportional to sum channel gain multiplied by error sensitivity, it is evident that all parameters are improved.

C. Primary Antenna Measurements

The ability of the 12-horn system to produce nearly equal edge illumination in the sum and difference modes is evident in the primary patterns (Figs. 7 and 8). This results in reasonably good performance of the sum channel without a degradation of the error sensitivity noted with the other systems. In order to minimize the horns in the feed, the individual horn apertures required were 1.5 wavelengths on a side. As is indicated in the H-plane pattern shown in Fig. 7(b), the first sidelobe is only −8 db as compared with the E-plane first sidelobe of −14 db.

It will be shown later that these high sidelobes are detrimental to the overall system gain and required corrective action.

Phase measurements of the comparator circuit that terminated in dummy loads indicated that null depths of −35 db in the azimuth plane and −25 db in the elevation plane could be expected. However, primary patterns show these preliminary data were in error since values of −47 and −35 db, respectively, were recorded.

All primary pattern measurements were taken at the Antenna Test Range in Bedford. The antenna mounted for primary patterns is shown in Fig. 9. The measurements included a check of the feed's response to circularly polarized signals. A rotating feed in an 8-foot paraboloid was used at the transmitting antenna. The feed spin rotation was kept below 15 rpm to eliminate possible pen-response errors in the recorder. Typical patterns taken in this manner are shown in Fig. 10. The axial ratio response to change in frequency is shown in Fig. 11.

Most primary pattern work was accomplished by utilizing three bolometer detector-recorder systems to obtain information simultaneously. Once the three systems were balanced out, this proved to be a timesaving method of collecting data.

Because there is a direct relationship between gain of the primary feed and system gain (i.e., a loss of 1 db in the feed will show up as a 1-db loss in the antenna), a careful investigation was made of the primary feed gain. By utilizing linear polarization, the gain measured in the transmit line was 19.1 db over isotropic. Theoretically, four linearly polarized horns, each 1.5 wavelengths on a side, should have 19.5 db gain; but with the horn flare angle used, a phase error of 0.125 wavelength exists over the radiating aperture of the horn reducing this value to 19.2 db, consistent with that actually measured. However, the orthogonal sum channel gain was 18.6 db, and when operating with circular polarization, the gain in both channels was 18.6 db.

After considerable investigation, it was shown that by inserting phase shifting dielectric blocks in four of the outside horns in order to change their termination, the gain was increased to 19.2 db. This same value was obtained by short circuiting the outside horns at their apertures. This indicated that coupling to these outside horns results in approximately a 0.6-db loss in gain. Provisions have been made to incorporate a modification in the system in order to eliminate this system loss.

The VSWR characteristics of the feed system are indicated in Fig. 12. Measurements were included at 1420 and 1670 Mcps in contemplation of work to be conducted at these frequencies, but no attempt had been made to match individual components since it was planned to use special matching devices when operating at these frequencies.

D. Secondary Pattern Results

Final testing was accomplished at the Millstone Hill radar site while transmitting from a source three miles away. Linear polarization was utilized with provisions made to rotate the polarization through 360°. Radiation pattern characteristics were within expectations. Refocusing of the subreflector optimized sum channel gain and the first sidelobe levels. Sum channel secondary patterns of the antenna system are shown in Figs. 13 through 15, and difference channel patterns are shown in Fig. 16. The first sidelobe levels of 16 to 17 db were also realized when the system was illuminated by a single pyramidal horn indicating that they were not necessarily due to the feed.

Primary pattern first sidelobes at approximately 30° [Fig. 7(b)] which become subreflector "spillover" in the secondary patterns can be seen in Fig. 13.

Nulls in the difference patterns were −32 db in the elevation plane and −35 db in the azimuth plane (Fig. 16). These nulls are not quite so deep as those of the primary patterns but are still very satisfactory for tracking purposes. They could be due to a slight misalignment of the center lines of the feed, subreflector, and main reflector, or because of the three-spar rather than the four-spar support.

The axial ratios of the transmit and orthogonal sum channels are 0.9 and 1.2 db, respectively. The circularity of polarization exists over all of the main beam and most of the first sidelobes.

Gain measurements of the antenna system were conducted using a 9-foot paraboloid with a waveguide feed as a gain standard. This unit was mounted behind the 84-foot main reflector on the roof of the equipment shelter. It was calibrated with a standard gain horn at the antenna range and found to have a gain of 27.1 db over isotropic. Figure 15 shows a main beam pattern with the gain standard pattern superimposed. A typical gain computation follows for the orthogonal sum port using circular polarization.

	Transmitted Polarization	
	Vertical	Horizontal
Gain standard over isotropic	27.1 db	27.1 db
Δ – difference between peaks	14.5	15.1
Line losses	1.2	1.2
	42.8 db	43.4 db
Power ratios*	19,050 +	21,880
	= 40,930	
	= 46.1 db	

Numerous recordings of gain were obtained in both sum channels. It was determined that the transmit sum gain was 46.5 ± 0.25 db and the orthogonal sum was 46.25 ± 0.25 db. Since these results were felt to be below the capabilities of the system, the following investigation was conducted by A.R. Dion on a single horn in an attempt to improve the antenna efficiency.

E. Modification to Improve Efficiency

The optimum efficiency of a Cassegrain antenna fed by a 4-horn monopulse arrangement is appreciably lower than that realized, for instance, with a single rectangular horn feed.[2] The principal factor contributing to the lower efficiency is the larger amount of spillover produced by the 4-horn feed. The spillover occurs principally in the direction of two broad sidelobes of relatively large amplitude (−8 db) as indicated in Fig. 7(b). These sidelobes can be reduced appreciably by placing metal septa parallel to the electric field at appropriate locations in the horn apertures (i.e., making the aperture illumination more uniform). With a proper choice of septum separations, the gain of one of the feed horns excited at its throat by a TE_{10} mode may be increased by about 0.9 db, which implies that its aperture efficiency may be increased to near unity. The investigation was carried out for a 4-horn array that propagates two orthogonally polarized modes with mutually perpendicular septa placed in their apertures. Their introduction in the horns results in an aperture configuration similar to a square array

*It can be shown that the gain of an elliptically polarized antenna is the sum of the power gain obtained with any two orthogonal polarizations.

of juxtaposed square horns. The normalized radiation pattern of a 4-horn monopulse feed (Fig. 17) is, to a good approximation,

$$E(\Theta, \varphi) = \frac{1 + \cos\Theta}{2} \left[\frac{\sin(u \cos\varphi)}{u \cos\varphi}\right] \left[\frac{\cos^2(\frac{u \sin\varphi}{2})}{1 - (u^2/\pi^2) \sin^2\varphi}\right] \tag{1}$$

where $u = (\pi d/\lambda) \sin\Theta$, and phase distribution of the aperture field is uniform. The corresponding power patterns in the two principal planes are plotted in Fig. 7 for the case where $d/\lambda = 1.515$, which is the size of the horn aperture in the 12-horn feed. The measured patterns also shown in Fig. 7 are in close agreement considering that an appreciable amount of phase error exists in the aperture field of these horns. The amount of power radiated in the direction of the two large sidelobes centered in the H-plane is appreciable and is lost as spillover. This spillover increases the level of the sidelobes of the secondary pattern in the same direction and reduces the antenna efficiency. The level of the two large sidelobes generated by the center four horns can be reduced appreciably by dividing the aperture of each horn into smaller apertures. The splitting of the field in the aperture of a square horn by means of orthogonal equispaced septa effectively produces an aperture field similar to that of a square array of identical square horns placed side by side. The resulting smaller apertures are assumed to be excited equally, which can be accomplished by a suitable choice of septum lengths. When the further assumptions are made that the field distribution in each aperture is identical to a TE_{10} mode, and that the currents flowing on the outside of the composite horn are negligible, the radiation field referred to the coordinate system of Fig. 17 is

$$E(\Theta, \varphi) = \frac{1}{N} \left(\frac{1 + \cos\Theta}{2}\right) \left[\frac{\sin(u \cos\varphi)}{u \cos\varphi}\right] \left[\frac{\sin(u \sin\varphi)}{\sin(\frac{u}{N} \sin\varphi)}\right] \left[\frac{\cos(\frac{u \sin\varphi}{N})}{1 - (4u^2/\pi^2 N^2) \sin^2\varphi}\right] \tag{2}$$

where $u = (\pi d/\lambda) \sin\Theta$, and N^2 is the number of square horns synthesizing the square aperture of side d. The aperture efficiency corresponding to this radiation field, i.e.,

$$\eta = \frac{1}{4(d/\lambda)^2 \int_{\Theta=0}^{\pi} \int_{\varphi=0}^{\pi/2} E^2(\Theta, \varphi) \sin\Theta \, d\Theta d\varphi} \tag{3}$$

is plotted as a function of N in Fig. 18 for the cases in which $d/\lambda = 8$, 4, and 3.0. The efficiency is seen to be nearly independent of the number of horns forming the aperture except in a narrow region where it increases rapidly from about 81 to about 100 percent. The rapid increase occurs at a value of N slightly larger than d/λ which corresponds to horn dimensions less than one wavelength on the side. Although the calculated efficiency is approximate and may be somewhat in error, it is reasonable to expect the change in efficiency to be accurate. Values of efficiency larger than unity should not be interpreted as erratic since this is entirely feasible for the small apertures (i.e., consider the limit when the horn becomes a slot).

The larger value of aperture efficiency occurs for horn side dimensions slightly less than one wavelength corresponding to a spacing between horn centers of the same magnitude. It is well known that a uniformly spaced array radiating a broadside beam, such as is the case here, generates grating lobes except for values of spacing less than one wavelength. The observed increase in efficiency therefore corresponds to the disappearance of these grating lobes. The

case shown in Fig. 18, where $d/\lambda = 3.03$, corresponds to the array of 1.5λ square apertures. It is observed that the efficiency of a square aperture of this size is close to unity when it is synthesized by 16 or more square horns. For the L-band feed, this efficiency can be realized by effectively dividing the aperture of each horn into four smaller horns. The addition of a cruciform septum inside a pyramidal square horn must result in four apertures with a pure or nearly pure TE_{10} mode field distribution and no or little cross-polarized components. The modes that exist in these apertures depend upon the septum length among other factors. This factor was studied experimentally by observing the radiation patterns of a square horn when septa of different lengths are placed inside its mouth. A horn of basic dimensions similar to those of the L-band feed horns was used. The dimensions of this horn and of the test septa are given in Fig. 19.

Septa of lengths ranging from $\frac{1}{8}$ inch to 6 inches were studied. The long septa were found to give rise to radiation patterns of nearly the expected configuration [Eq. (1)] but also give rise to a large amount of cross-polarized radiation such that the addition of the cruciform septum actually reduced the aperture efficiency. The very short septum, on the other hand, did not give rise to cross-polarized radiation but did not produce as sharp an H-plane beamwidth as did the longer ones and therefore resulted in efficiencies less than optimum. Septum lengths between $\frac{3}{4}$ inch and $1\frac{1}{2}$ inches result in radiation patterns close to expectation with an acceptable level of cross-polarized radiation (−23 db). The addition of a septum inside a horn gives rise to a reflected wave of larger amplitude for the longer septa. For the modification, $\frac{3}{4}$-inch-long septa were chosen; the reflected wave set up by this obstacle produces a VSWR of about 1.6. This mismatch was reduced by adding two orthogonal $\frac{1}{8}$-inch rods in line with the septa about $\lambda/4$ in front of them.

The increase in gain resulting from the addition of the cruciform septum in the mouth of the horn was measured by comparison with a standard gain horn and was also obtained by pattern integration. In both cases an increase of 1.0 db was obtained, a value slightly larger than expected. However, calculations were carried out for horn apertures free of phase errors, which is not the actual case; the addition of the septum "straightens" the wave to some degree and thus reduces the gain loss resulting from phase deviations in the aperture. Patterns comparing horns, with and without septa, are shown in Fig. 20.

With this information it was decided to modify the existing horns. Although the modification was only needed in the four center horns, it was placed in all twelve. This prevented disturbing the good phase relationship known to exist, as is evident by the excellent difference patterns realized.

Installation of the septated horns resulted in a gain of 47.4 ± 0.25 db in the transmit sum channel, an increase of 0.9 db, and an efficiency of 46 percent. The orthogonal sum channel gain increased to 46.9 ± 0.25 db. This corresponds to an increase of 0.65 db and an efficiency of 41 percent. Thus both channels realized an increase in gain only slightly less than that calculated. Sidelobes at ≈30° (Fig. 13) were reduced from −36.8 to −39 db. Difference pattern characteristics were not appreciably altered by this modification.

Although the gain figures and tolerances allowed do overlap, it would be presumptuous to say that the two gains are actually equal. When the number of readings taken is considered, it is apparent that the orthogonal sum gain is lower by approximately 0.5 db. This difference can be attributed to the coupling between horns which was discovered during primary pattern work.

When operating with circular polarization, it was determined that the two gains were low but equal. A difference was noted between the two gains when the system was operated as a dual linearly polarized system. But the determining factor in all cases is the phase relationship between the primary radiation and that radiation coupled to the outside horns, reflected and reradiated. As the point of reflection is changed, the relative phase changes and this in turn alters the gain in each sum channel. Stub tuners could be installed at those points in the comparator where signals from the outside horns are added to the center horn signal. By proper tuning, the phase of the coupled signal could be altered so that the reradiated signal combines properly with the signal radiated from the center four horns. This would most certainly tend to increase the antenna efficiency.

F. VSWR and Isolation Measurements

Various measurements of the VSWR of the feed system and connecting transmission lines were obtained. The transmit sum channel, measured at the hybrid input, is 1.20. A special sweep bend with inductive iris reduced this VSWR to 1.07 at 1295 Mcps. The receive lines were measured in the equipment shelter and included several waveguide straight sections and bends and the $1\frac{5}{8}$-inch coaxial rotary joints. The VSWR of the orthogonal sum channel was 1.18 at 1295 Mcps, and under 1.40 over the 100-Mcps band (1250 to 1350). The azimuth difference was under 1.20 over the entire band, while the elevation difference line was 1.5:1 over the band.

The isolation between the sum and the orthogonal sum channels is 27 db. This level, determined by the inherent isolation of the transducer and the mismatch at the transducer output, was adequate protection for the receive TR switches.

III. REFLECTOR SYSTEM

A Cassegrain optics reflector system was imperative in this application because of the size and complexity of the feed itself. Supporting the feed at the apex would be an insurmountable mechanical problem. However, three advantages in using the Cassegrain principle are:

(a) Accessibility to the feed.
(b) Shorter transmission lines between receiver and antenna.
(c) Flexibility in the choice of f/D ratio.

The primary reflector is a full paraboloid 84 feet (112 wavelengths) in diameter. The surface is constructed of perforated surface modular panels, the perforations being $\frac{1}{4}$ inch in diameter located on $\frac{3}{8}$-inch center lines. Individual panels are separated by no more than $\frac{1}{4}$ inch. The surface tolerance was designed for ±0.250 inch peak-to-peak, and measurements indicate an RMS value of 0.122 inch. The focal length is 25 feet (f/D of 0.3).

The secondary reflector is a solid aluminum hyperboloid, 10 feet in diameter mounted by three aluminum support spars. The subreflector tolerance of ±0.050 inch was obtained. The angle subtended by the subreflector at the feed is 29°, and the nominal distance from the vertex of the subreflector to the feed aperture is $17\frac{1}{2}$ feet (Fig. 3). The magnification factor is 7.0. Positioning of the subreflector for alignment and focusing is accomplished by the movement of three large adjustment bolts behind the hyberbola.

IV. TRANSMISSION LINES

Transfer of energy from transmitter to the azimuth rotary joint is accomplished through a WR-770 waveguide. A WR-650 waveguide connects this joint to the TR switch, the elevation rotary joint, and the four center horns of the feed horn array.

It was found that when operating at high average power levels (over 100 kw), considerable electrical breakdown was experienced in the transmit waveguide between the azimuth rotary joint and the feed. With high peak power and a reduced pulse width, no breakdown was evident (5-Mw peak with 0.1-μsec pulse width instead of 0.33 μsec). Various modifications to the system reduced the frequency of these discharges (i.e., replacement of mitered bends with sweep bends and replacement of flexible waveguides which had relatively high VSWR's), but the problem was never completely eliminated. Eventually, the entire WR-650 waveguide run including the rotary joints was replaced with WR-770 sections. Although again reducing the frequency of breakdown, the problem still exists, and to insure continuous operation, the waveguide is filled with the dielectric gas sulfur hexafluoride.

The receive lines consist of WR-650 waveguide except for short sections in the elevation torque tube where $1\frac{5}{8}$-inch coaxial rotary joints are used. These lines are terminated in the equipment shelter where the received signals are converted to an intermediate frequency. The signals are then routed through $\frac{3}{8}$-inch-diameter heliax coaxial lines and "around-the-mast" rotary joints located on the azimuth axis to the receiver room at ground level.

V. AUXILIARY CIRCUITS AND FEED COMPONENTS

A. Auxiliary Circuits

Additional low-power RF circuits were added to aid in operating and maintaining the system (Fig. 21). For example, dipole antennas to simulate off-axis targets during calibration of the tracking system are mounted on the subreflector. These antennas are half-wave dipoles, each of which is connected to a $\frac{7}{8}$-inch coaxial line whose other terminals are open circuited. Directional couplers (30 db) and RG-9/U cables are used to couple the antennas to the receiving equipment through a remotely controlled single-pole 4-throw coaxial switch. The switch is used to allow selection of any one of three dipole antennas. It allows the transmission of a low-power signal through the appropriate dipole.

The transmit waveguide line has two bi-directional couplers strategically located to monitor transmitted power levels in the areas adjacent to the rotary joints. They aid in determining the position of any high power breakdown and constantly monitor the VSWR in the line.

A power monitor is also included at the input to the comparator by taking advantage of the inherent isolation of the difference arm of an E-plane hybrid. Instead of terminating this unused port, the signal received is cabled back to a power meter in the equipment shelter. This signal is 35 db below that of the transmitted signals: 30 db contributed by the hybrid isolation, and 5 db by the cable used.

A TR protective circuit is included where the usually loaded port of the TR assembly is cabled to the equipment shelter. If the energy level in this line exceeds a preset value, it indicates a malfunction in the TR and a circuit is triggered shutting down the transmitter.

B. Feed Components

1. Rotary Joints

Since the antenna must be capable of rotating 360° in azimuth and 90° in elevation, two identical high power rotary joints (Fig. 22) are provided. They are single-channel units that use the TM_{01} circular waveguide mode. (Because of the high average power used, and the complexity of a cooling system for the inner conductor, it was decided not to use the conventional coaxial door-knob transition-type rotary joint.) Each unit consists of two well-matched transitions from rectangular to circular waveguide separated by a length of circular waveguide. The rotary section is located in the circular waveguide and consists of a conventional arrangement of RF chokes. The VSWR at 1300 Mcps is 1.07 and varies approximately 1.05 as a function of rotation (Fig. 23). The phase variation is the relative shift of field minimums measured in guide wavelengths.

Pressurized $1\frac{5}{8}$-inch coaxial joints (Fig. 24) are used in the elevation axis to transfer the receive signals from the antenna to the equipment shelter. The joints have a VSWR under 1.10 over a 10-percent band and use noncontacting RF chokes.

Four around-the-mast rotary joints (Fig. 25) operating at 105 Mcps transfer the intermediate frequency signals through the azimuth axis. One additional joint operating at 150 Mcps is used in transmitting local oscillator signals from the receiver room to the equipment shelter. The insertion phase variation as a function of rotation is less than 0.1° on all these units.

2. E- and H- Tuner

The tuner is a conventional WR-770 waveguide magic T. The E- and H-arms contain remotely controlled double-bucket sliding-short plungers. The faces of the plungers were water cooled because high temperatures were contemplated in this area, but subsequent tests indicated that the surface temperatures did not exceed those experienced in other sections of guide. Consequently, the radar operates without use of the water-cooling system. The tuner position is controlled by a balanced-bridge helipot servo system. Total travel of the plungers is 10 inches with a bucket position reset capability of approximately ±0.010 inch.

3. Polarizer

The polarizer section is a 14-inch-long section of 6- × 6-inch-ID square waveguide. It is located between dual-polarization transducers and the horns in the feed system. When operating with linear polarization, this square waveguide section is all that is required. However, in the circular polarization mode of operation, these sections must be replaced by square waveguide sections which contain metallic loading in the diagonal corners (Fig. 26). The incident wave, vertically polarized in the transmit case, may be resolved into two waves E_1 and E_2 (Fig. 27) which are in phase, of equal intensity, and orthogonally polarized. By wedge loading the diagonal corners of the square waveguide, a relative phase shift is produced between these two waves.[3,4] By altering the height and length of the wedges, it is possible to realize a 90° relative phase shift, thus producing circular polarization. The ideal design would use extremely long wedges which protrude only slightly into the waveguide. This provides a small phase shift per unit length (requiring the longer length) but does not introduce a high mismatch into the system as would be realized with larger wedges. Space limitation, however, prevented the use of wedge length in excess of one guide wavelength. Circular polarization was realized with a wedge height

of 1-7/32, but because of the mismatch introduced at the transducer output, the isolation between the transmit sum and orthogonal sum channels was reduced to 21 db. By introducing a slightly higher step in the middle of the wedge, the match was improved and the isolation was increased to −27 db. The overall height of the wedge had to be reduced to 1/16 of an inch in order to again realize circular polarization, because adding the step increased the relative phase shift to more than 90°.

4. Radome

The feed is protected from the weather by a 3/16-inch-thick single-piece Rexolite radome (Fig. 28). The radome face, which is 6-1/2 feet in diameter, has six 1-inch-thick stiffening members to reduce deflection due to the 1000-lb force exerted by the 1/4-psi internal pressure. Rexolite was used for the radome material because of its inherent low loss (dissipation factor 0.00054, dielectric constant 2.5), allowing it to accommodate the power output capability of the transmitter. Tests conducted on both a high heat resistant nylon and a special low-loss fiberglass resulted in radome burnouts. The single-piece construction required the casting of, what is believed to be, the largest piece of Rexolite ever attempted.

5. Miscellaneous Components

The dual polarization transducer (Fig. 29) separates the receive energy into two orthogonally polarized signals. The measured VSWR of this unit is shown in Fig. 30. The isolation between the two orthogonal ports was 35 db when the transducer was terminated in a 1.015:1 matched load. This isolation decreases as the mismatch seen by the transducer increases (i.e., that contributed by the polarizer, horn, and subreflector). The isolation experienced in the final system is 25 db.

An E-plane hybrid was developed (Fig. 31) that provides 40-db isolation between sum and difference ports and VSWR's as indicated in Fig. 32.

Mitered E- and H-plane 90° bends were also designed; almost 30 units are needed in the comparator alone. Their performance characteristics are shown in Fig. 33.

Design of E- and H-plane power dividers, 45° offsets, and a Y power divider was also necessary in the comparator assembly. Typical VSWR curves of the Y magic T and the Y H-plane power divider (Fig. 29) are shown in Figs. 34 and 35, respectively.

VI. CONCLUSION AND RECOMMENDATIONS

Conversion of the Millstone Hill radar to an L-band 12-horn monopulse tracker has been completed. The predicted improvement in tracking sensitivity over a 4-horn monopulse system is apparent. The antenna efficiency of 46 percent in the transmit sum channel is equivalent, within one or two percent, to that obtained with a theoretically optimum 4-horn Cassegrain monopulse system,[2] assuming 0.6-db loss due to aperture block and surface inaccuracy. Performance of the system to date indicates a complete justification of the added effort needed in the construction of a 12-horn rather than a 4-horn system.

The one disadvantage noted, which does not exist in a 4-horn system performance, is the lower efficiency of the orthogonal sum channel caused by the coupling of energy to the outside horns. In a 12-horn system design, provision should be made to adjust the phase of this coupled energy in order to insure maximum efficiency in all channels. This corrective action usually has no adverse effect on other performance characteristics of the system.

ACKNOWLEDGMENTS

The assistance of the following members of Lincoln Laboratory is gratefully acknowledged: Mr. L. J. Ricardi for his advice and encouragement throughout; Mr. E. W. Blaisdell for his cooperation and assistance on the major mechanical problems; Mr. L. G. Kraft for his suggestions and assistance in the early design considerations; Messrs. W. C. Pineo and H. H. Danforth and others of Group 31 who assisted in testing the complete system; Dr. A. R. Dion for his work on the modification of the horns and design of the around-the-mast rotary joint; Dr. R. N. Assaly and those members of Groups 61 and 71 involved in the extensive development effort of the entire system conversion.

REFERENCES

1. L. J. Ricardi and L. Niro, "Design of a Twelve-Horn Monopulse Feed," Group Report 315G-0002, Lincoln Laboratory, M. I. T. (24 March 1961).
2. A. R. Dion, "The Aperture Efficiency of Some Horn-Fed Paraboloidal Reflectors," Group Report 61G-3, Lincoln Laboratory, M. I. T. (30 December 1963), DDC 431779, H-566.
3. R. N. Assaly, "The Guide Wavelength of Cylindrical Waveguide of Arbitrary Cross Section and a Computer Program for Calculating Values," Technical Report 313, Lincoln Laboratory, M. I. T. (20 May 1963), DDC 412518.
4. A. H. Kessler and W. J. Getsinger, "A Simple Method for Designing An Elliptical Polarizer in Square Waveguide," Group Report 46G-3, Lincoln Laboratory, M. I. T. (28 May 1963), DDC 407624, H-514.

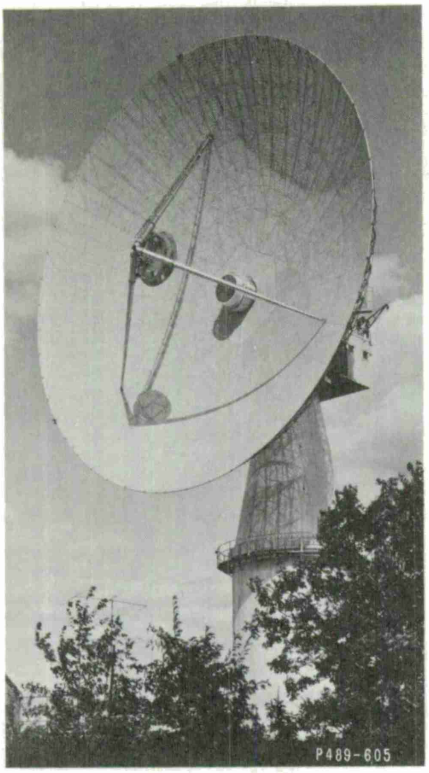

Fig.1. Millstone Hill L-band radar.

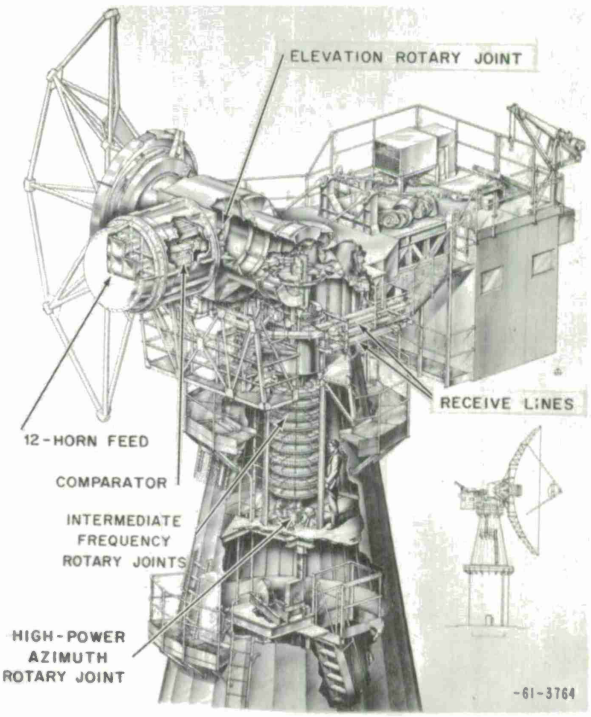

Fig. 2. Cutaway of Millstone radar.

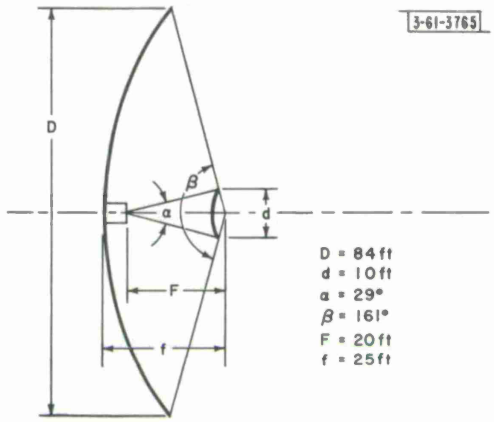

Fig. 3. Geometry of Millstone radar antenna.

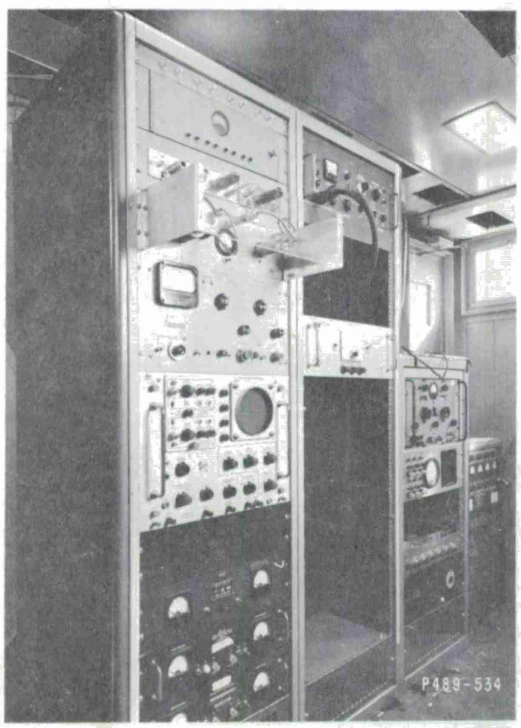

Fig. 4. Equipment shelter.

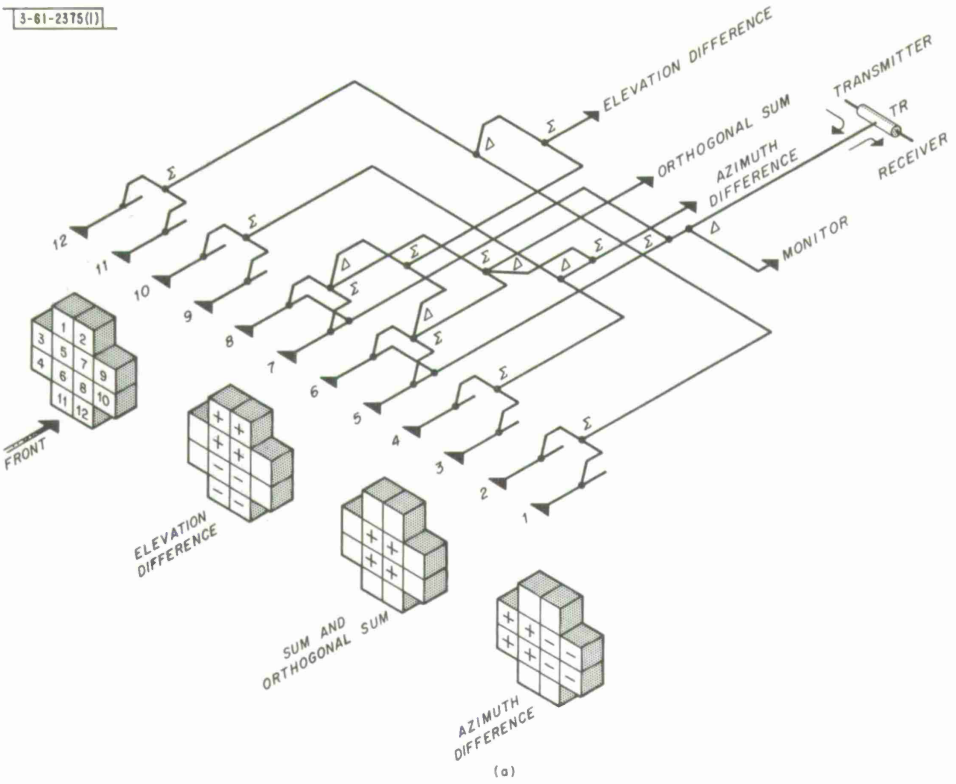

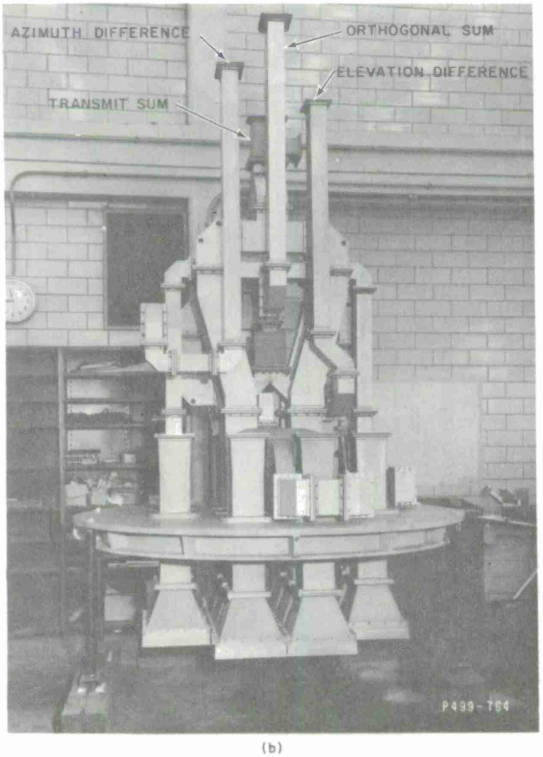

Fig.5(a-b). 12-horn comparator.

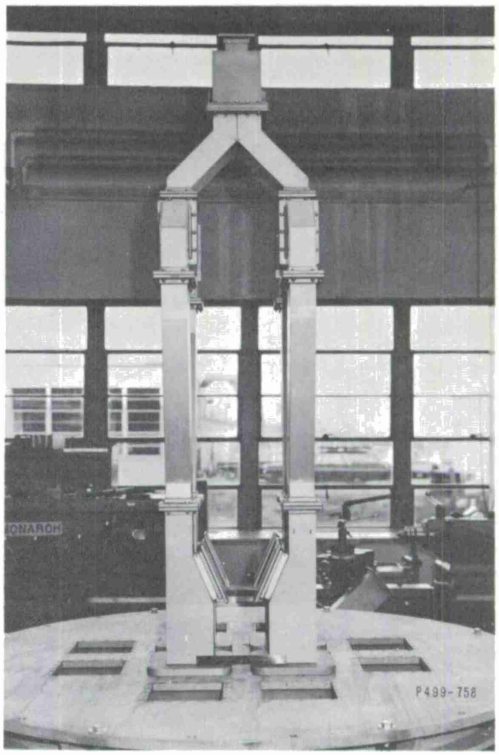

(a) Side view.

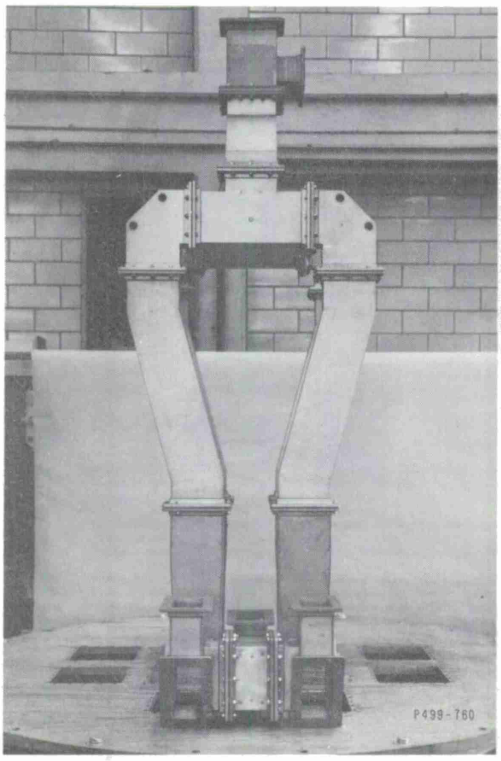

(b) Top view.

Fig. 6(a-b). Transmit sum channel.

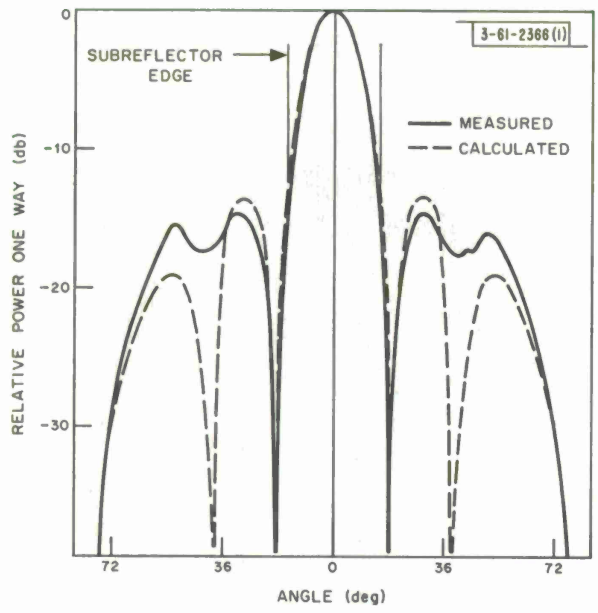

(a) E-plane.

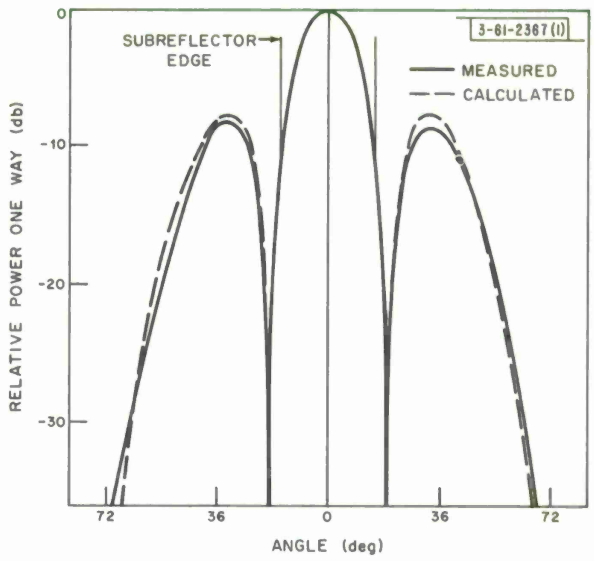

(b) H-plane.

Fig. 7(a-b). Primary patterns, sum channel (1295 Mcps).

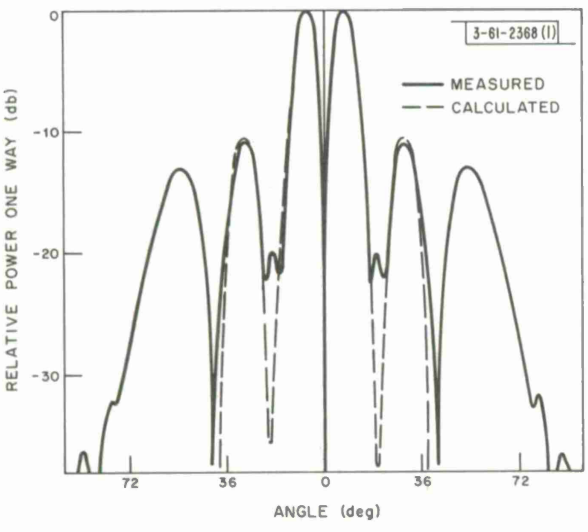

(a) Azimuth.

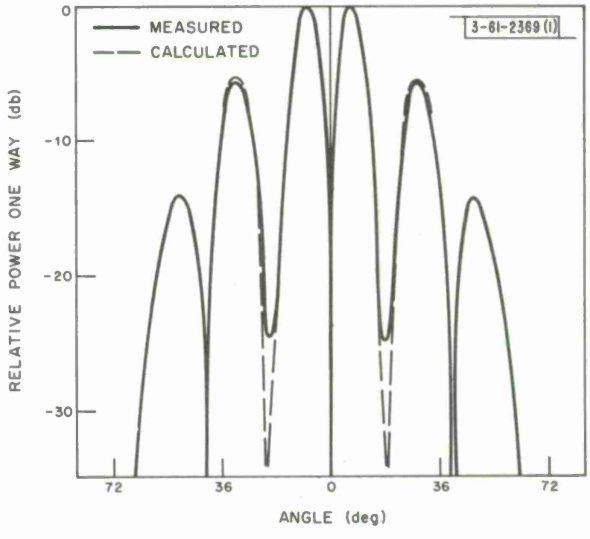

(b) Elevation.

Fig. 8(a-b). Primary patterns, difference channels (1295 Mcps).

(a) Rear view.

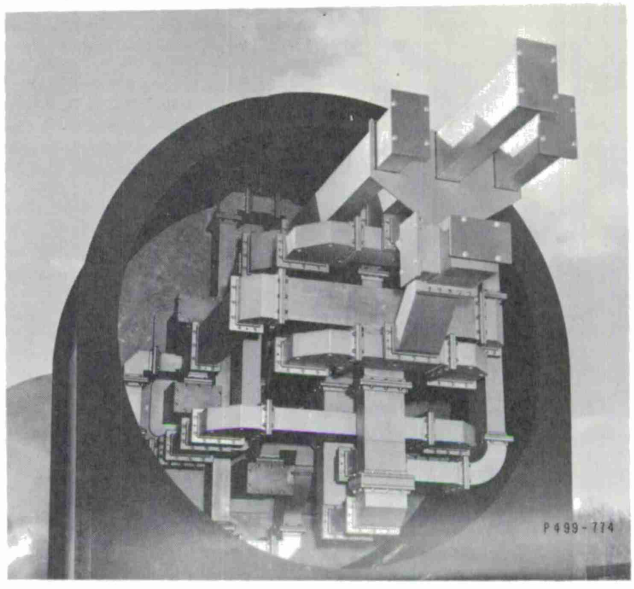

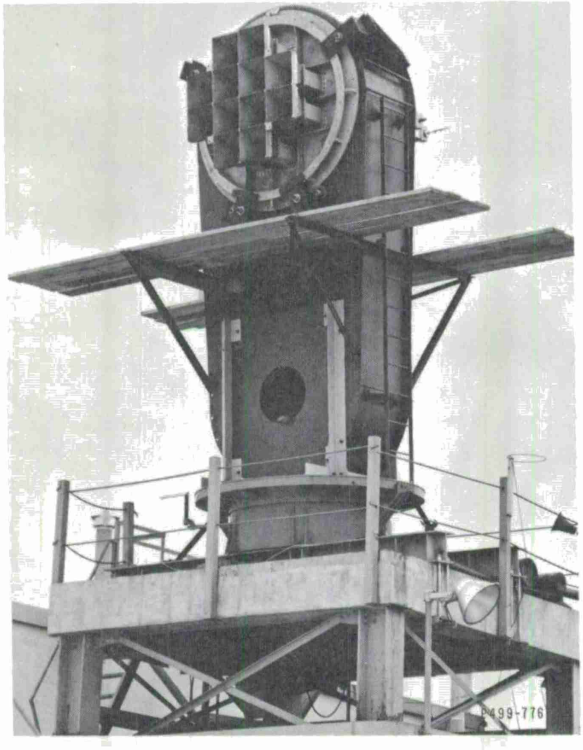

(b) Front view.

Fig. 9(a-b). Feed under test.

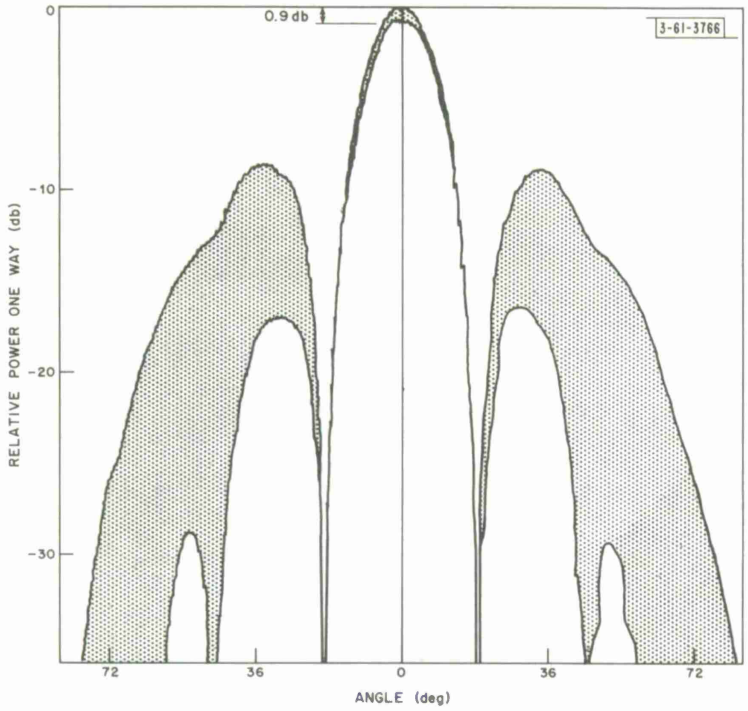

(a) Transmit.

(b) Orthogonal.

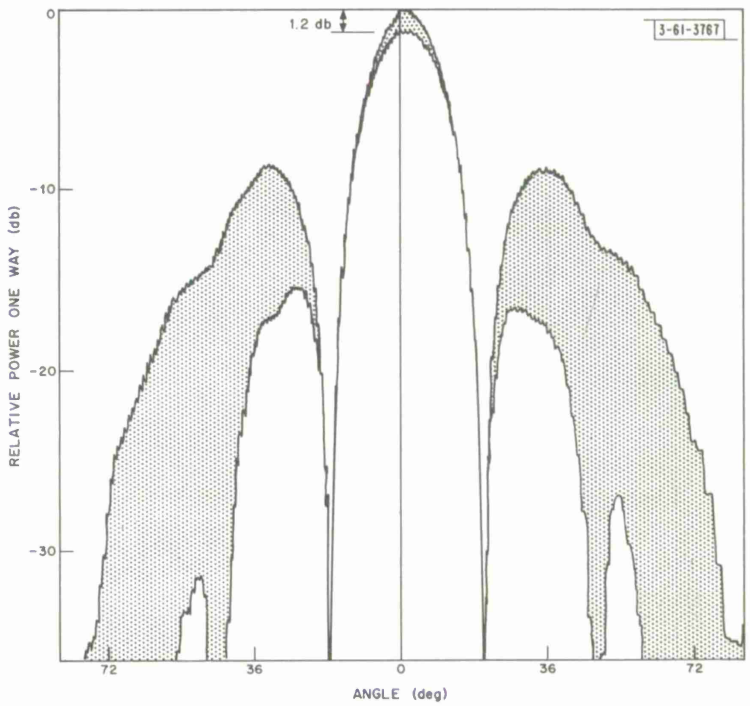

Fig. 10(a-b). Axial ratio patterns, sum channels (1295 Mcps).

Fig. 11. Primary pattern axial ratio (1295 Mcps).

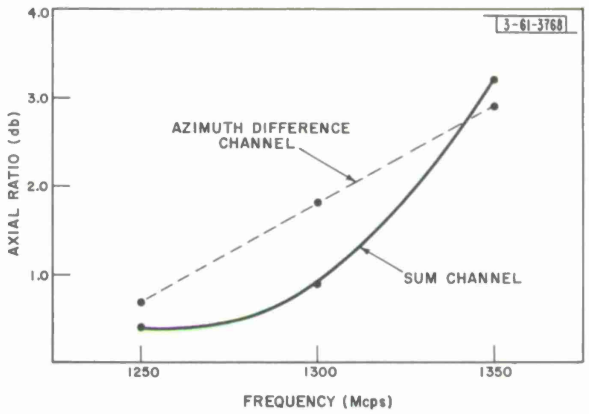

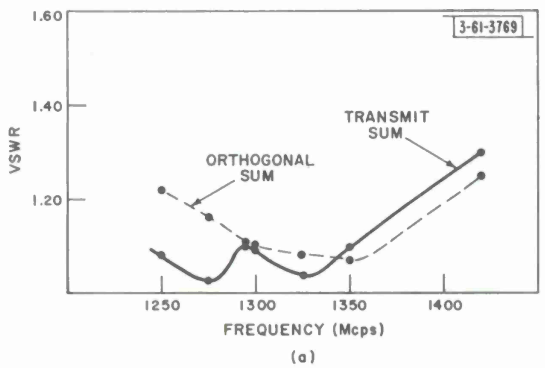

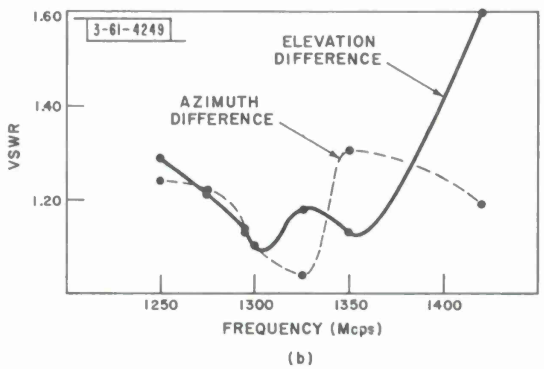

Fig. 12(a-b). Comparator VSWR graphs.

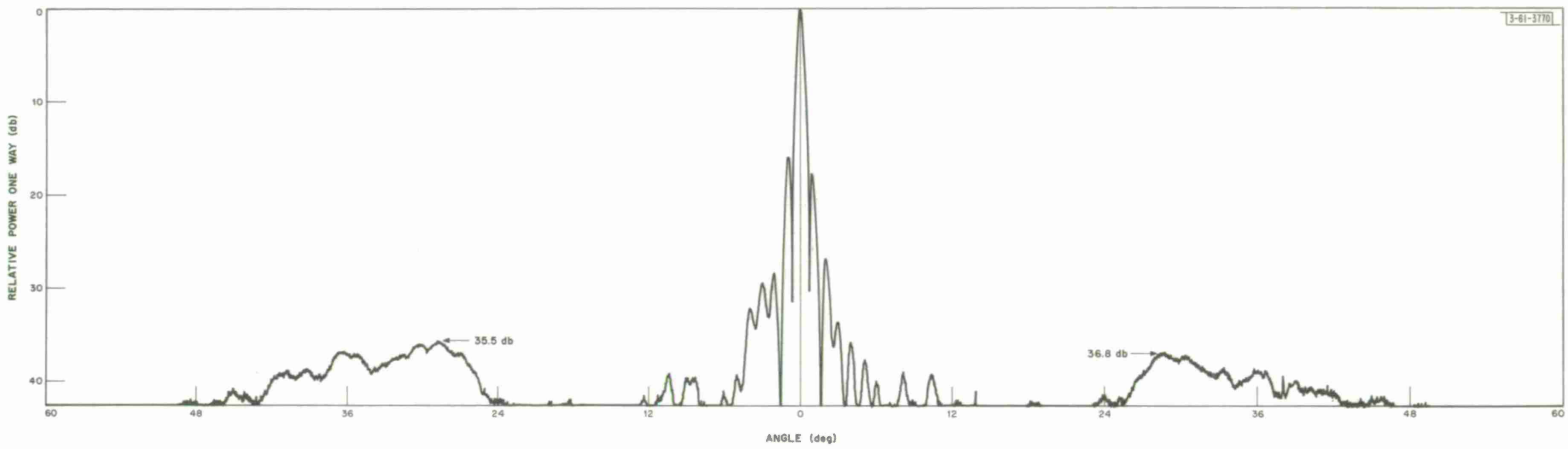

Fig. 13. Secondary pattern, H-plane sum channel, ±60° (1295 Mcps).

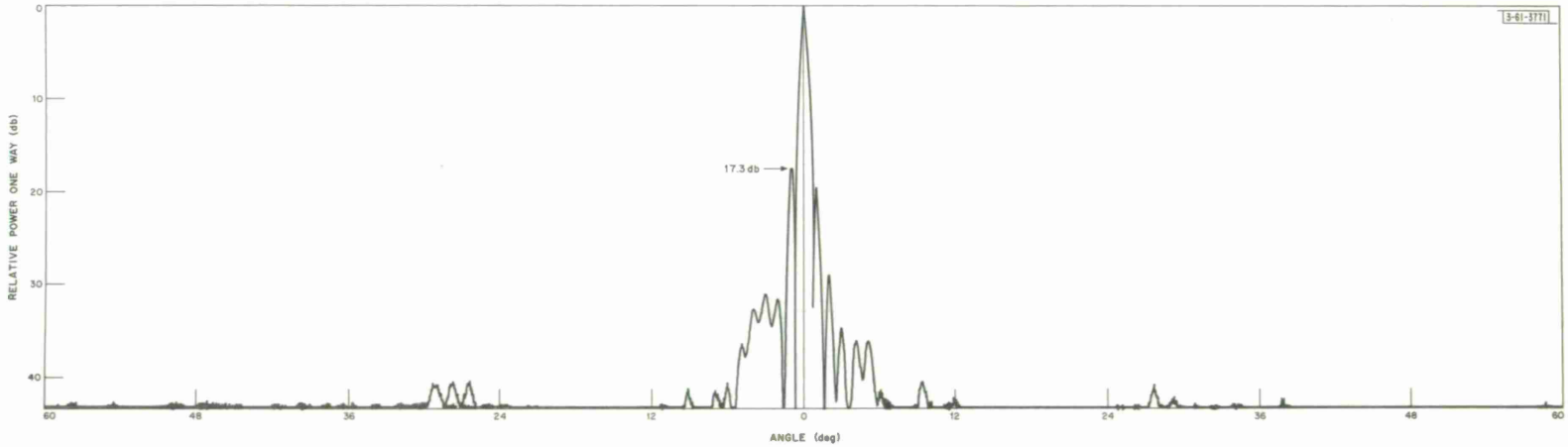

Fig. 14. Secondary pattern, E-plane sum channel, ±60° (1295 Mcps).

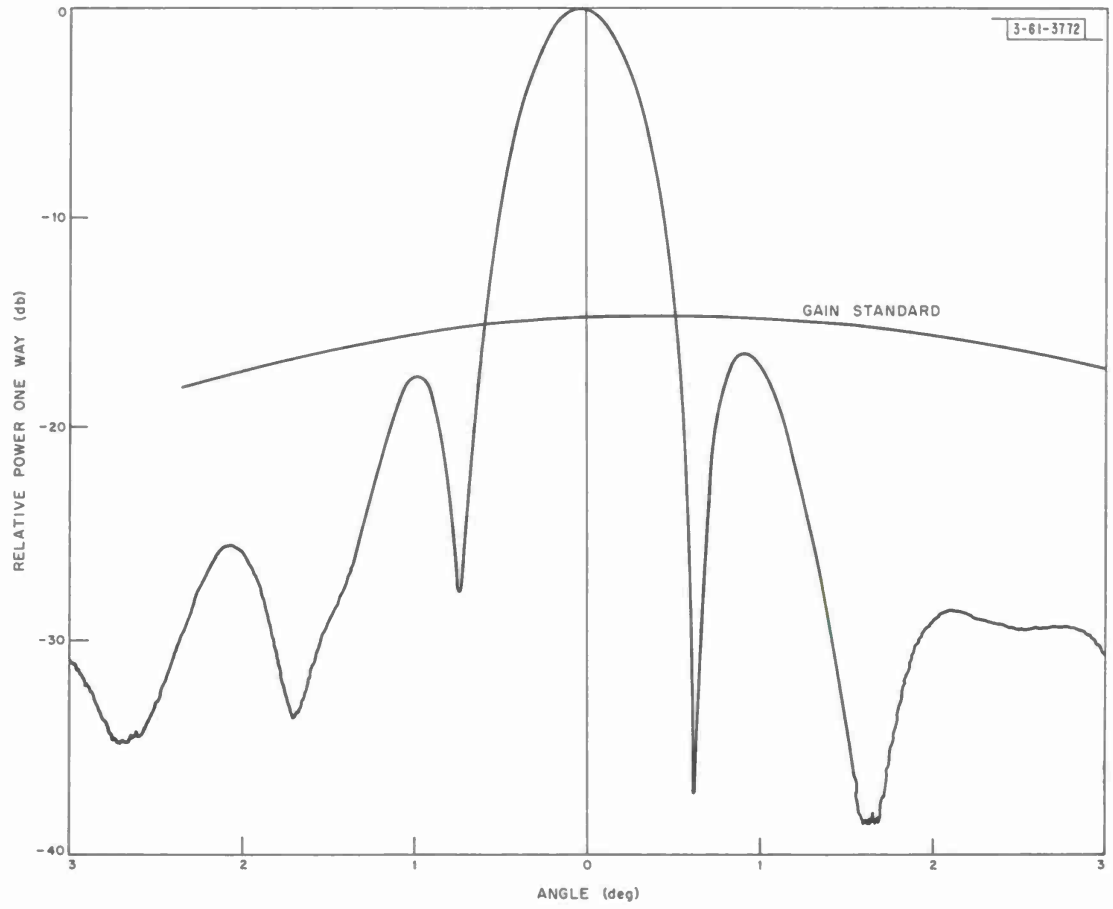

Fig. 15. Secondary pattern, orthogonal sum (1295 Mcps).

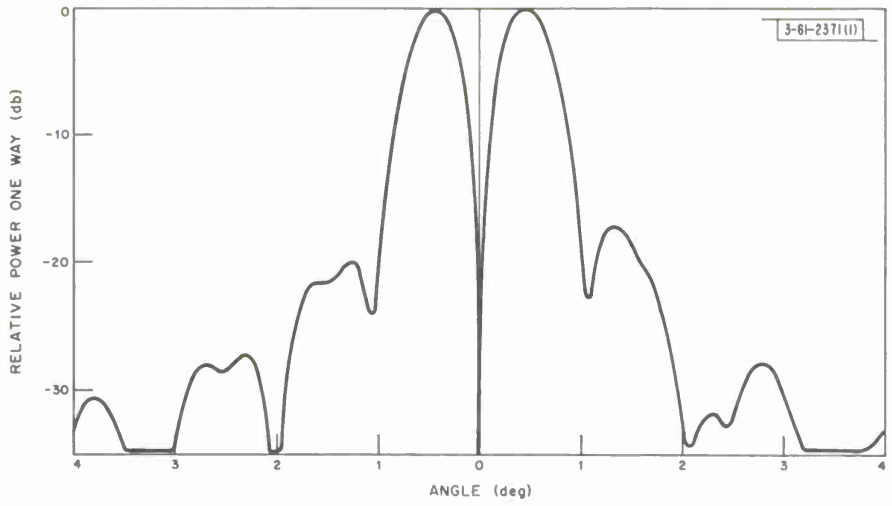

(a) Azimuth.

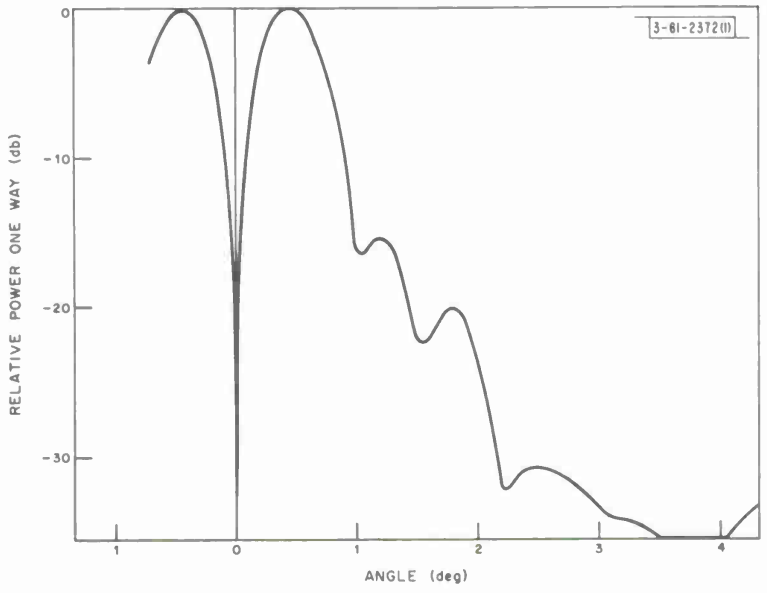

(b) Elevation.

Fig. 16(a-b). Secondary patterns, difference channels (1295 Mcps).

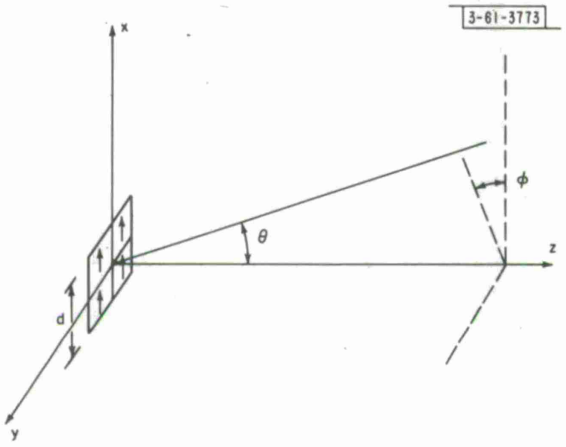

Fig. 17. 4-horn coordinate system.

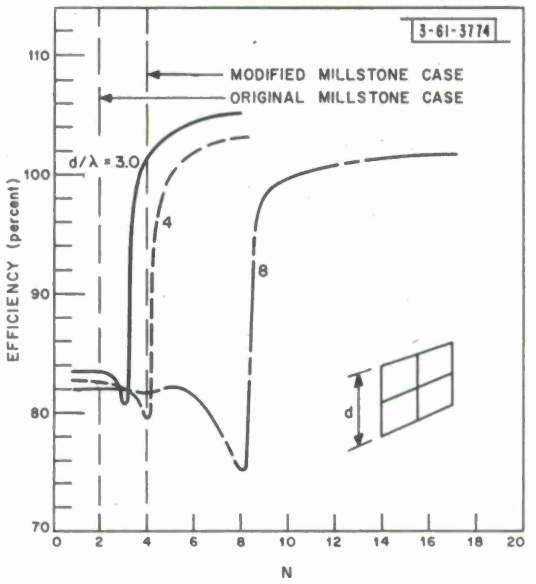

Fig. 18. Aperture efficiency of an array of square horns.

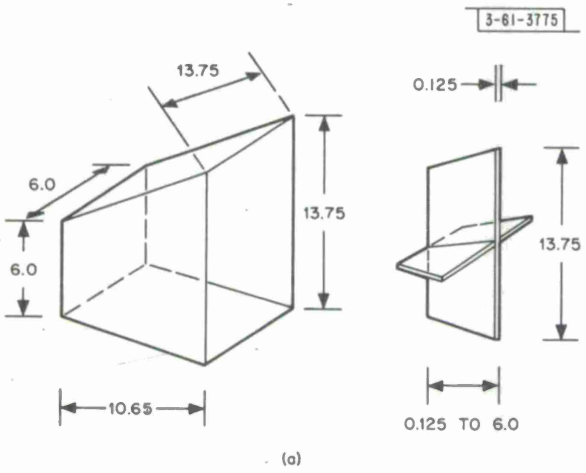

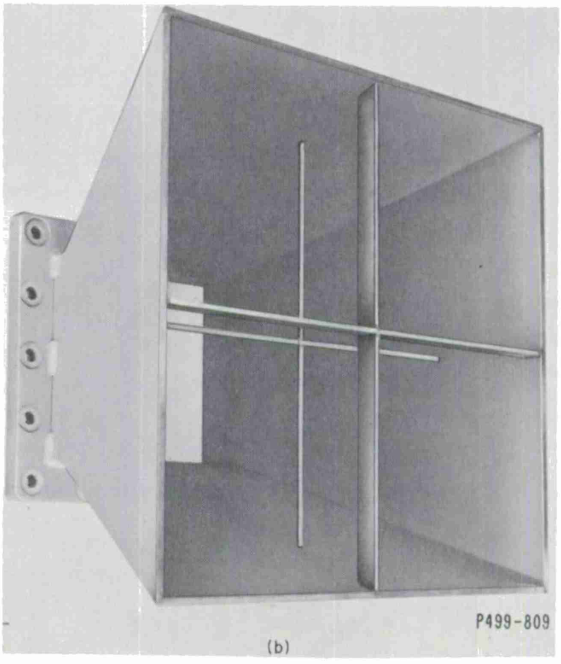

Fig. 19(a-b). Septated feed horn (dimensions in inches).

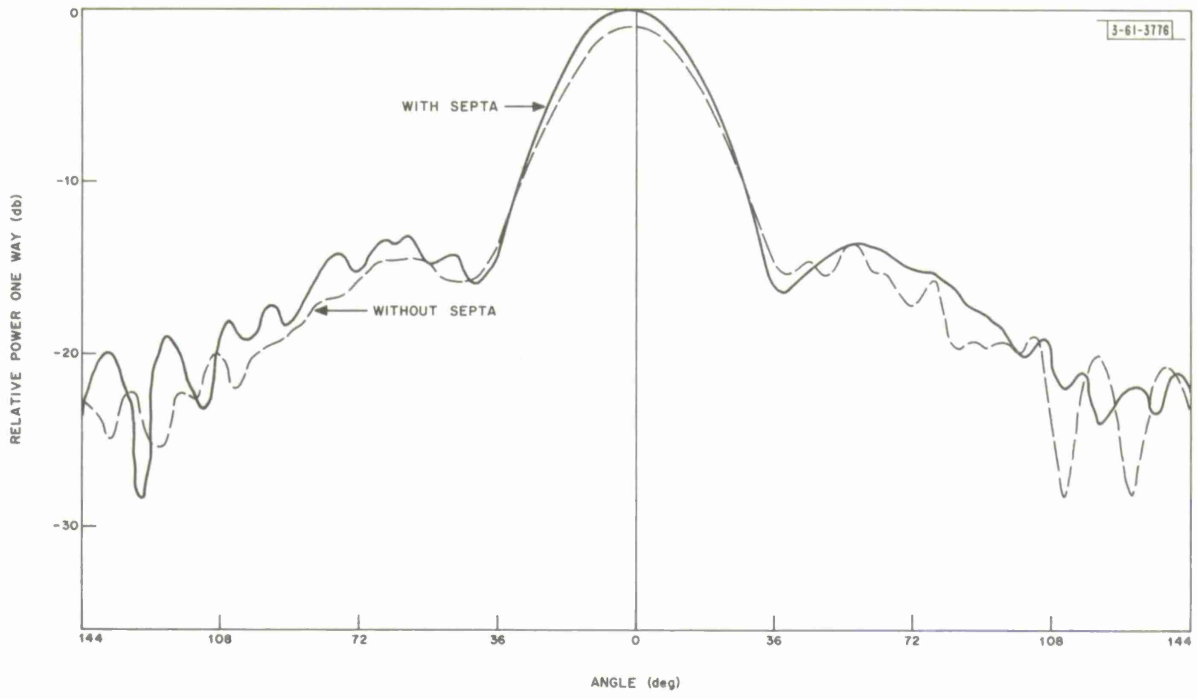

(a) E-plane.

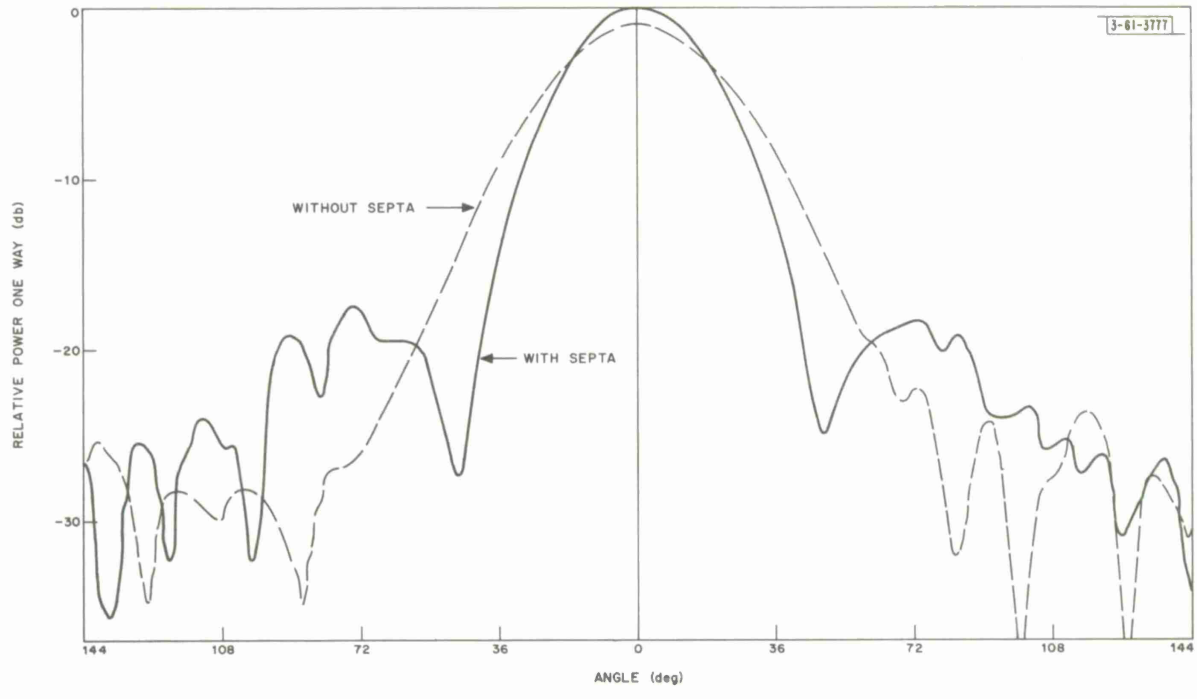

(b) H-plane.

Fig. 20(a-b). Radiation patterns, single 1.5 λ square horn.

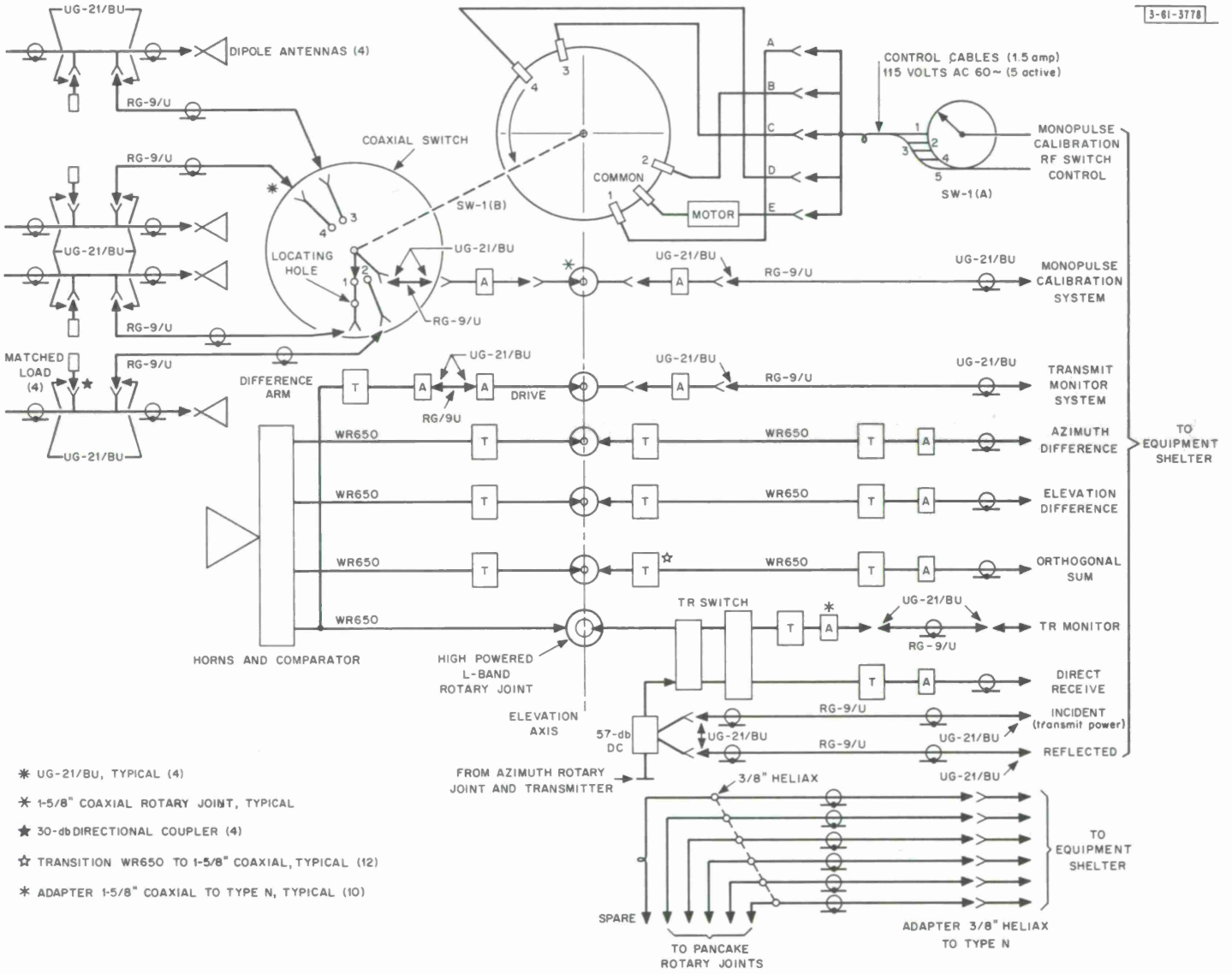

Fig. 21. Auxiliary circuit schematic.

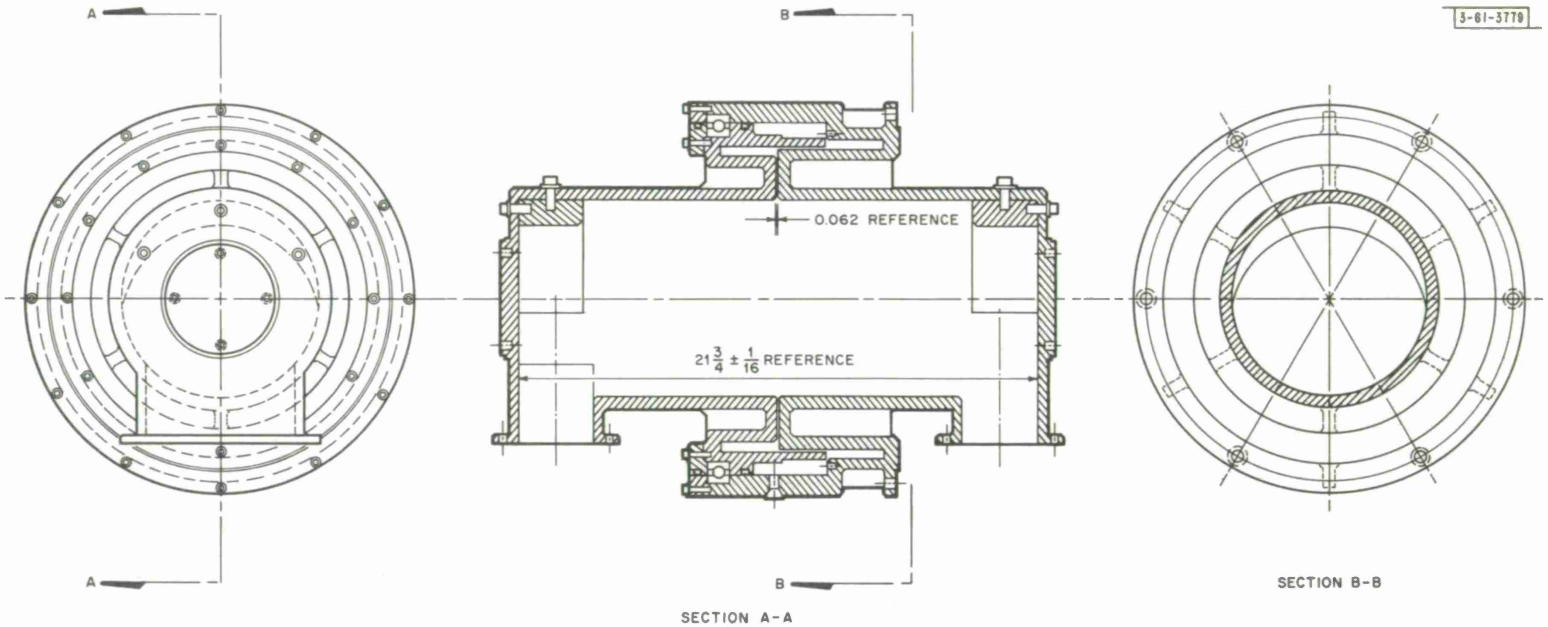

Fig. 22. High power WR-650 rotary joint.

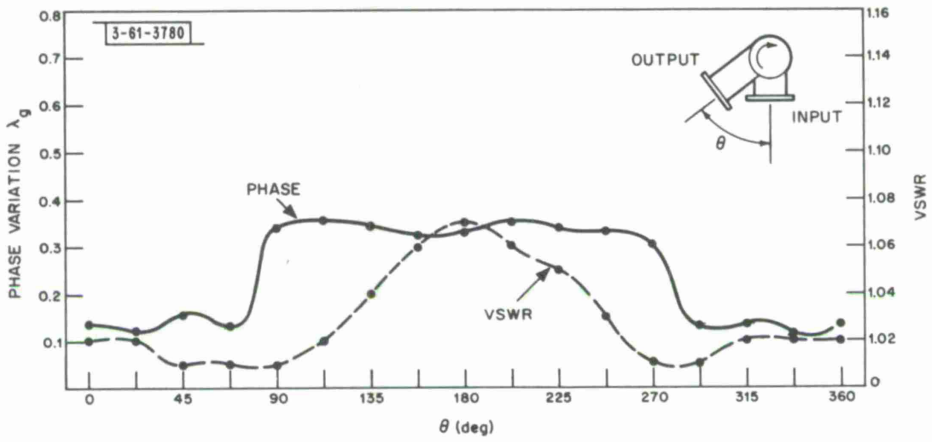

Fig. 23. High power rotary joint VSWR and phase variation (1300 Mcps).

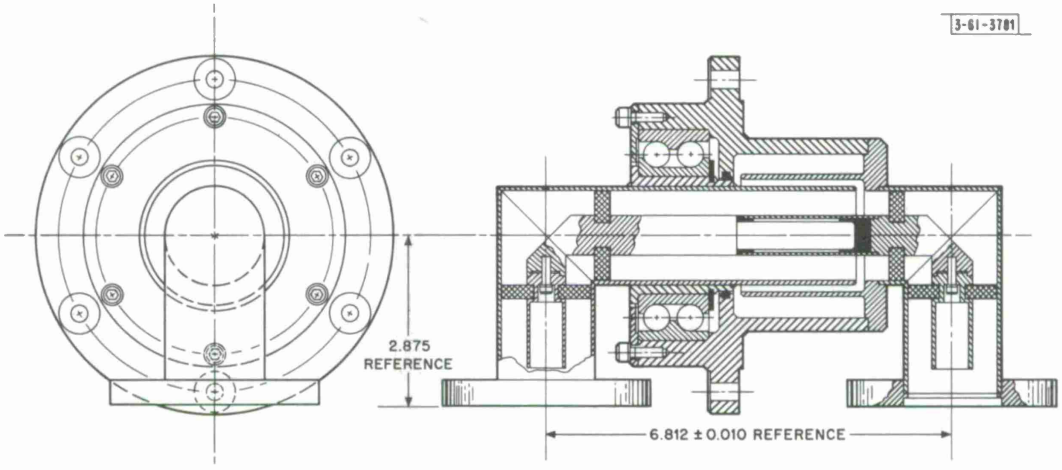

Fig. 24. Diagram of 1-5/8-inch coaxial rotary joint.

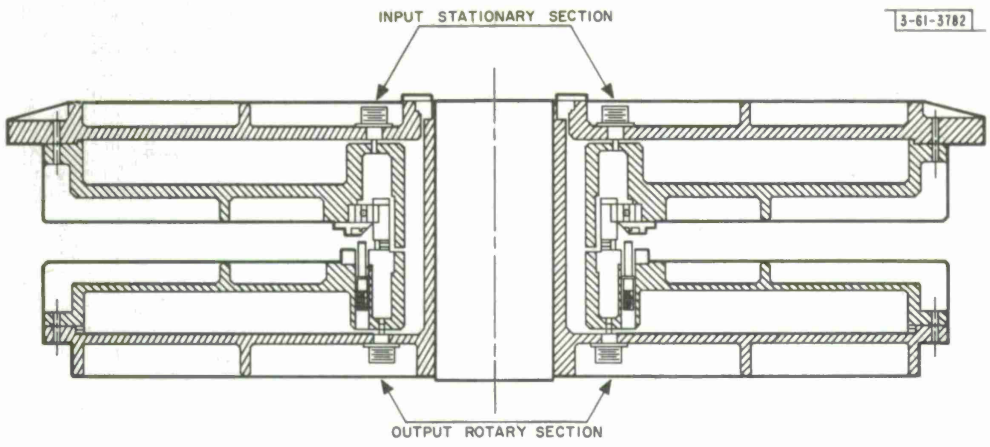

(a)

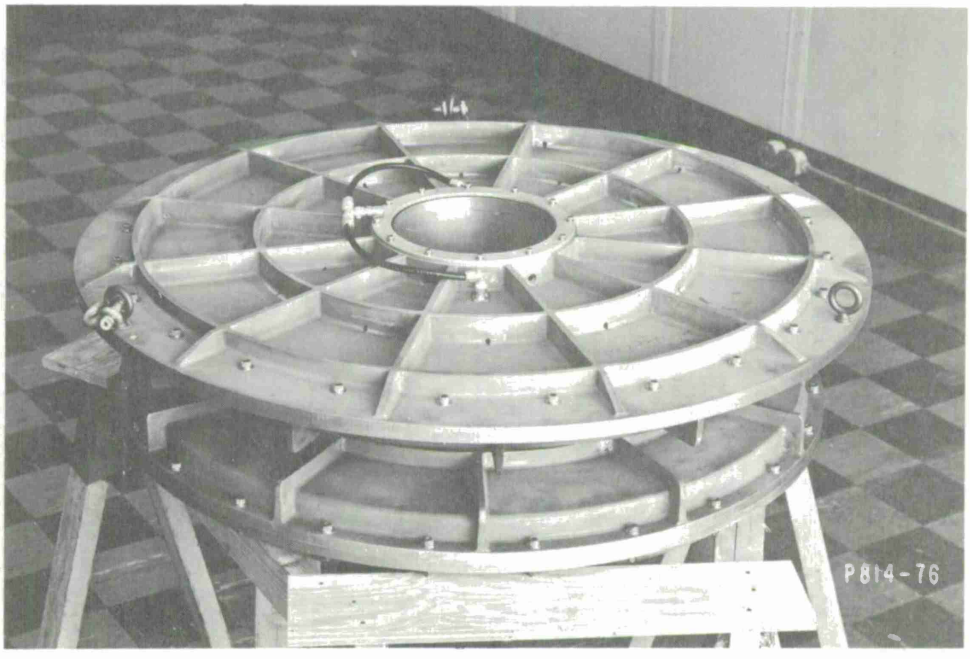

(b)

Fig. 25(a-b). 105- and 150-Mcps pancake rotary joint.

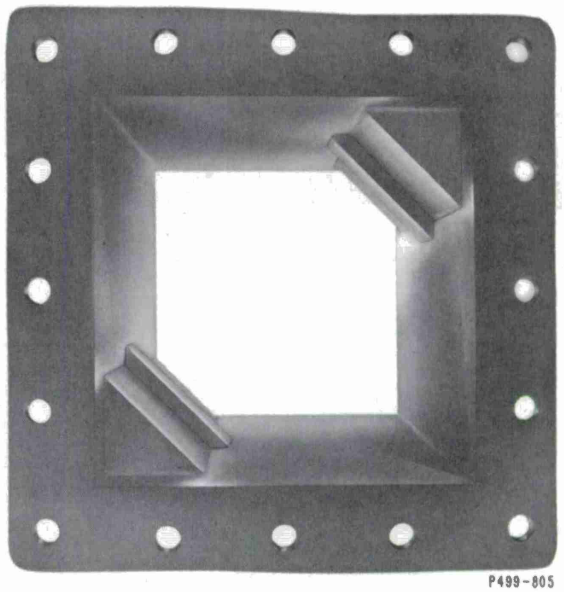

Fig. 26. Waveguide circular polarizer.

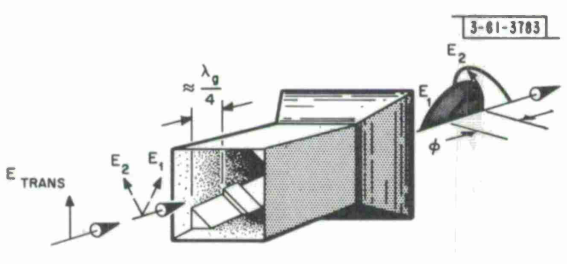

(a) Transmit: RHCP.

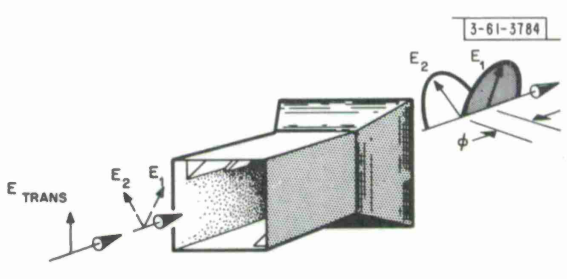

(b) Transmit: LHCP.

Fig. 27(a-b). Polarizer schematic.

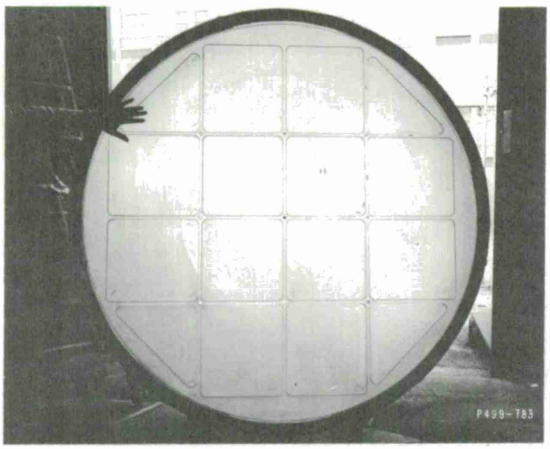

Fig. 28. Radome.

Fig. 29. Polarization transducer and H-plane power divider.

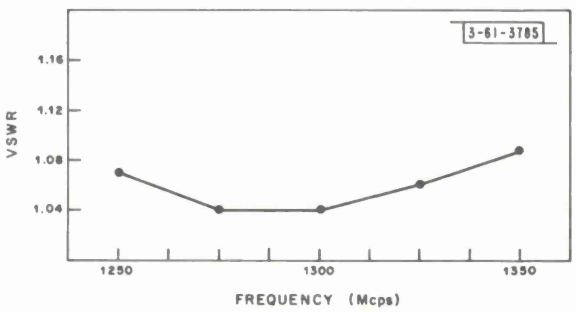

(a) Transmit sum arm.

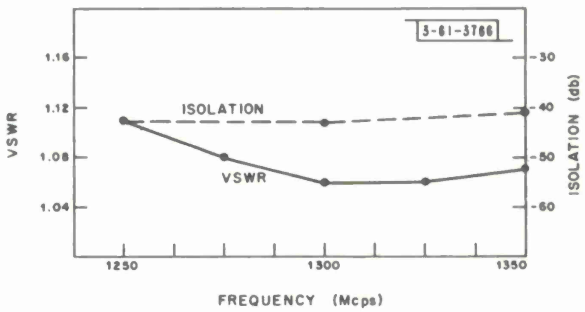

(b) Orthogonal sum arm.

Fig. 30(a-b). Polarization transducer VSWR curves.

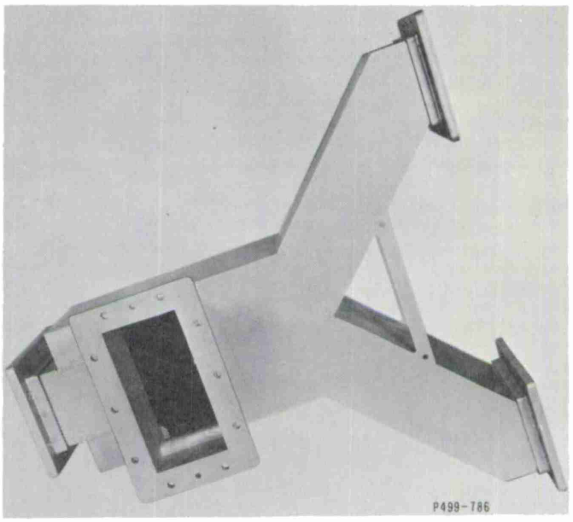

Fig. 31. E-plane hybrid.

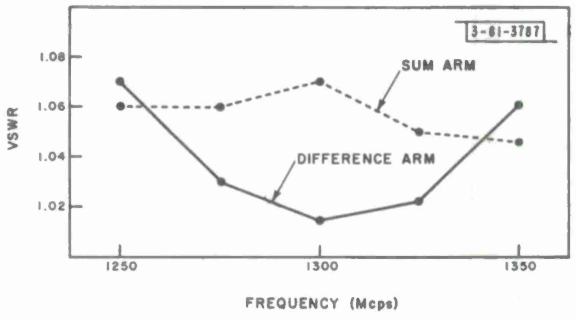

Fig. 32. E-plane hybrid VSWR curves.

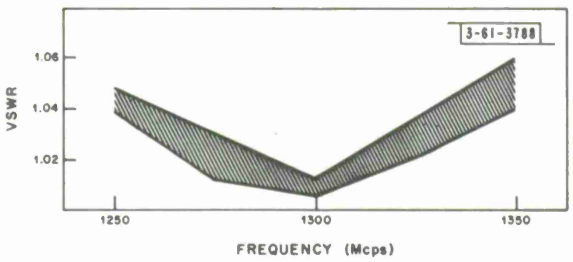

(a) H-plane.

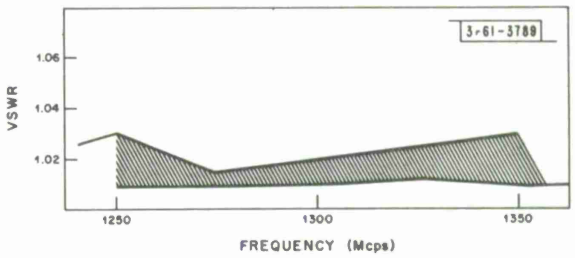

(b) E-plane.

Fig. 33(a-b). Mitered 90° bends VSWR curves. Curves show range of VSWR for all bends tested.

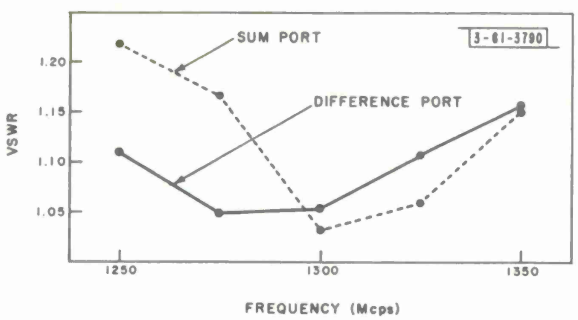

Fig. 34. Y magic T VSWR curves.

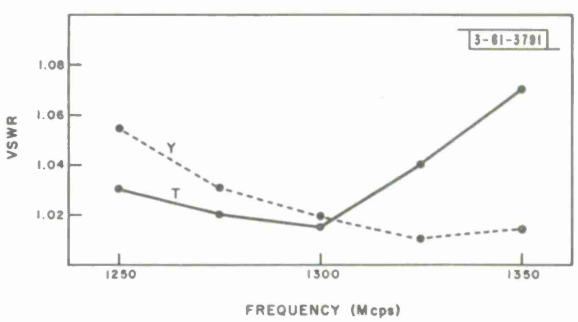

Fig.35. Y H-plane power divider VSWR curves.

DOCUMENT CONTROL DATA – R&D

(Security classification of title, body of abstract and indexing annotation must be entered when the overall report is classified)

1. ORIGINATING ACTIVITY *(Corporate author)*
Lincoln Laboratory, M.I.T.

2a. REPORT SECURITY CLASSIFICATION
Unclassified

2b. GROUP
None

3. REPORT TITLE
12-Horn Monopulse Antenna System for Millstone Hill Radar

4. DESCRIPTIVE NOTES *(Type of report and inclusive dates)*
Technical Report

5. AUTHOR(S) *(Last name, first name, initial)*
Lindberg, Charles A.

6. REPORT DATE
15 June 1965

7a. TOTAL NO. OF PAGES
40

7b. NO. OF REFS
4

8a. CONTRACT OR GRANT NO.
AF 19(628)-500

b. PROJECT NO.
649L

c.

d.

9a. ORIGINATOR'S REPORT NUMBER(S)
Technical Report 393

9b. OTHER REPORT NO(S) *(Any other numbers that may be assigned this report)*
ESD-TDR-65-238

10. AVAILABILITY/LIMITATION NOTICES
None

11. SUPPLEMENTARY NOTES
None

12. SPONSORING MILITARY ACTIVITY
Air Force Systems Command, USAF

13. ABSTRACT

The 440-Mcps conical-scan tracker at the Millstone Hill radar site has been converted to an L-band 12-horn monopulse tracker utilizing a Cassegrain optics reflector system. The amplitude sensing monopulse feed illuminates a 10-foot subreflector and thence an 84-foot diameter paraboloid with linear or either sense of circular polarization. This system conversion increased the capabilities of the radar complex in that higher antenna gain and increased tracking sensitivity are obtained. The merits of the 12-horn system have been proved with actual results substantiating the theoretical predictions. This report discusses the design considerations and final performance characteristics of the overall antenna system and its individual components.

14. KEY WORDS

radar
Millstone Radar
monopulse antenna system
Cassegrainian system
tracking antenna
L-band

Printed by
United States Air Force
L. G. Hanscom Field
Bedford, Massachusetts